

Singlet Oxygen in a Cell: Spatially Dependent Lifetimes and Quenching Rate Constants

Marina K. Kuimova,^{*,†,§} Gokhan Yahioglu,^{†,‡} and Peter R. Ogilby^{*,§}

Chemistry Department, Imperial College London, Exhibition Road, London SW7 2AZ, U.K.,
PhotoBiotics Ltd., 21 Wilson Street, London EC2M 2TD, U.K., and Center for Oxygen
Microscopy and Imaging, Department of Chemistry, University of Aarhus,
Århus DK-8000, Denmark

Received September 20, 2008; E-mail: m.kuimova@imperial.ac.uk; progilby@chem.au.dk

Abstract: Singlet molecular oxygen, $O_2(a^1\Delta_g)$, can be created in a single cell from ground-state oxygen, $O_2(X^3\Sigma_g^-)$, upon focused laser irradiation of an intracellular sensitizer. This cytotoxic species can subsequently be detected by its 1270 nm phosphorescence ($a^1\Delta_g \rightarrow X^3\Sigma_g^-$) with subcellular spatial resolution. The singlet oxygen lifetime determines its diffusion distance and hence the intracellular volume element in which singlet-oxygen-initiated perturbation of the cell occurs. In this study, the time-resolved phosphorescence of singlet oxygen produced by the sensitizers chlorin (Chl) and 5,10,15,20-tetrakis(*N*-methyl-4-pyridyl)-21*H*,23*H*-porphine (TMPyP) was monitored. These molecules localize in different domains of a living cell. The data indicate that (i) the singlet oxygen lifetime and (ii) the rate constant for singlet oxygen quenching by added NaN_3 depend on whether Chl or TMPyP was the photosensitizer. These observations likely reflect differences in the chemical and physical constituency of a given subcellular domain (e.g., spatially dependent oxygen and NaN_3 diffusion coefficients), thereby providing evidence that singlet oxygen responds to the inherent heterogeneity of a cell. Thus, despite a relatively long intracellular lifetime, singlet oxygen does not diffuse a great distance from its site of production. This is a consequence of an apparent intracellular viscosity that is comparatively large.

Introduction

Singlet oxygen, $O_2(a^1\Delta_g)$, is the lowest excited state of molecular oxygen.^{1–3} It is well-established that singlet oxygen is an oxidizing/oxygenating agent for a wide range of organic molecules.^{1,4} Production of sufficient quantities of singlet oxygen in a biological environment can perturb cellular processes and ultimately cause cell death via apoptosis or necrosis.^{5,6} The cytotoxic effect of singlet oxygen is currently used in clinical practice in a treatment modality called photodynamic therapy (PDT), whereby the controlled production of singlet oxygen leads to the eradication of undesired tissue.⁷ Singlet oxygen production also forms part of many natural signaling pathways and is often an important response to stress in mammalian and plant cells.^{8–11}

A common and convenient way to produce singlet oxygen is photosensitization.² In this process, a molecule (the so-called sensitizer or, in the case of PDT, the added drug) absorbs light to populate an excited state. Most efficient sensitizers readily produce a long-lived triplet state that transfers its energy of excitation to the ground state of molecular oxygen, $O_2(X^3\Sigma_g^-)$, in a collision-dependent process. Quenching of a sensitizer excited state by $O_2(X^3\Sigma_g^-)$ to produce $O_2(a^1\Delta_g)$ kinetically competes with sensitizer fluorescence and phosphorescence. Under most circumstances, the latter are sufficiently probable, even in the presence of oxygen, to provide a convenient optical probe of the sensitizer.

Arguably, the most unambiguous way to monitor singlet oxygen is by direct observation of its phosphorescence ($a^1\Delta_g \rightarrow X^3\Sigma_g^-$) at 1270 nm. Although this phosphorescence is weak ($\phi \approx 10^{-7}$), we have shown that it can nevertheless be detected from a single cell in both steady-state and time-resolved experiments upon irradiation of a sensitizer incorporated into the cell.^{12–16} A key aspect of our work is that using a focused laser beam allows sensitizer excitation to be confined to small

[†] Imperial College London.

[‡] PhotoBiotics Ltd.

[§] University of Aarhus.

- (1) Foote, C. S.; Clennan, E. L. In *Active Oxygen in Chemistry*; Foote, C. S., Valentine, J. S., Greenberg, A., Liebman, J. F., Eds.; Chapman and Hall: London, 1995; pp 105–140.
- (2) Schweitzer, C.; Schmidt, R. *Chem. Rev.* **2003**, *103*, 1685–1757.
- (3) Paterson, M. J.; Christiansen, O.; Jensen, F.; Ogilby, P. R. *Photochem. Photobiol.* **2006**, *82*, 1136–1160.
- (4) Clennan, E. L.; Pace, A. *Tetrahedron* **2005**, *61*, 6665–6691.
- (5) Weishaupt, K. R.; Gomer, C. J.; Dougherty, T. J. *Cancer Res.* **1976**, *36*, 2326–2329.
- (6) Redmond, R. W.; Kochevar, I. E. *Photochem. Photobiol.* **2006**, *82*, 1178–1186.
- (7) Bonnett, R. *Chemical Aspects of Photodynamic Therapy*; Gordon and Breach Science Publishers: Amsterdam, 2000.

- (8) Ledford, H. K.; Niyogi, K. K. *Plant Cell Environ.* **2005**, *28*, 1037–1045.

- (9) Klotz, L.-O. *Biol. Chem.* **2002**, *383*, 443–456.
- (10) Klebanoff, S. J. *J. Leukocyte Biol.* **2005**, *77*, 598–625.
- (11) Steinbeck, M. J.; Khan, A. U.; Karnovsky, M. J. *J. Biol. Chem.* **1992**, *267*, 13425–13433.
- (12) Zebger, I.; Snyder, J. W.; Andersen, L. K.; Poulsen, L.; Gao, Z.; Lambert, J. D. C.; Kristiansen, U.; Ogilby, P. R. *Photochem. Photobiol.* **2004**, *79*, 319–322.
- (13) Skovsen, E.; Snyder, J. W.; Lambert, J. D. C.; Ogilby, P. R. *J. Phys. Chem. B* **2005**, *109*, 8570–8573.

subcellular spatial domains.^{15,17,18} Through the use of this approach, it is now possible to provide unique insight into singlet-oxygen-mediated processes that occur in a cell.

The lifetime of singlet oxygen depends significantly on the surrounding environment and also exhibits characteristically large solvent isotope effects.² In our work on single cells to date, we have exploited the latter to enhance the intensity of the singlet oxygen phosphorescence signal detected. Specifically, the lifetime of singlet oxygen is $\sim 67 \mu\text{s}$ in D_2O ¹⁹ but only $\sim 3.5 \mu\text{s}$ in H_2O ,²⁰ and this difference is manifested in the quantum efficiency of singlet oxygen phosphorescence.^{2,21} In view of this, we routinely work under conditions in which the intracellular H_2O has been exchanged with D_2O . Most importantly, we have demonstrated that this $\text{H}_2\text{O}/\text{D}_2\text{O}$ exchange does not affect cell viability over the time course of our experiments.¹⁶

In most of our previous singlet oxygen work in cells, we used a hydrophilic cationic porphyrin as a photosensitizer: 5,10,15,20-tetrakis(*N*-methyl-4-pyridyl)-21*H*,23*H*-porphine (TMPyP). This molecule tends to accumulate in the nucleus of a cell, but an appreciable amount can still be found in the cytoplasm.^{14,22,23} Time-resolved singlet oxygen phosphorescence experiments performed on D_2O -incubated, TMPyP-containing cells yield an intracellular singlet oxygen lifetime of $\sim 30\text{--}40 \mu\text{s}$, irrespective of whether the data are recorded from the cytoplasm or the nucleus.^{13–16} As expected on the basis of the known solvent isotope effect (see above), this lifetime is progressively shortened for cells with an increasing ratio of intracellular H_2O to D_2O and extrapolates to a value of $\sim 3 \mu\text{s}$ in a cell containing H_2O .^{15,16}

It is now well-established that “apparent” diffusion coefficients of small molecules inside a cell can be appreciably smaller than those in a homogeneous aqueous or hydrocarbon solvent.²⁴ This includes the apparent diffusion coefficient of intracellular oxygen.^{25–28} The data recorded point to a value for the oxygen diffusion coefficient that could be up to 1 order of magnitude smaller than that in bulk water at 25 °C. It is important to note that given the heterogeneity of a cell and the differences in the spatial resolution of the techniques used to quantify the translational motion of oxygen, it is appropriate to speak of an average or “apparent” value for the intracellular

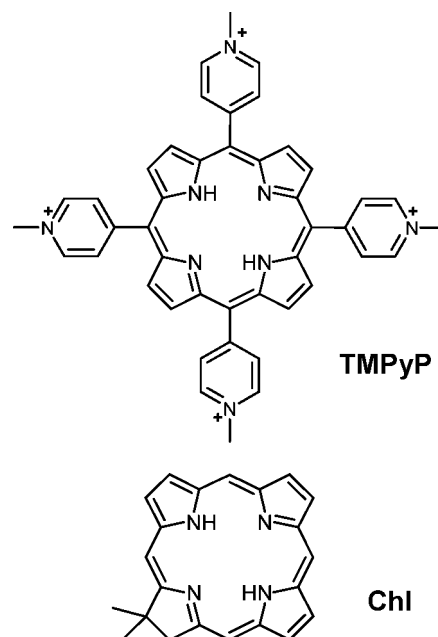


Figure 1. Structures of the photosensitizers used in this study.

diffusion coefficient. The comparatively small values of intracellular diffusion coefficients are consistent with independent data that point to subcellular domains that can be quite viscous.²⁹

For the present study, we set out to record singlet oxygen data that reflected the heterogeneity of a single cell. On one hand, we were interested in seeing if we could obtain spatially dependent lifetimes of singlet oxygen that might reflect the unique chemical composition of a given domain. Thus far, direct evidence for subcellular spatially dependent differences in singlet oxygen lifetimes has not been presented. On the other hand, we wanted to ascertain if the rate constant for the quenching of singlet oxygen by an added molecule likewise depended on the subcellular domain that was probed. For the latter study, the chemical composition of a given domain is not as important as the diffusion rate of species in that domain (i.e., the viscosity of the local environment). To support this intracellular quenching study, we performed control experiments using sucrose solutions to examine the effects of a viscosity change on the quenching rate constant and thereby establish a reference framework for data recorded from a cell.

A key premise in our experiments is the fact that the intracellular environment is highly heterogeneous, and since the intracellular diffusion coefficient of oxygen can be small, one could create populations of singlet oxygen confined to selected subcellular domains. Although we can impart spatial resolution to our experiments by irradiating the sensitizer in the cell with a focused laser, our present beam waist (diameter $\approx 1 \mu\text{m}$)^{15,18} is still large relative to the structures that define intracellular heterogeneity. Thus, we chose to work with both hydrophobic [chlorin (Chl)] and hydrophilic (TMPyP) sensitizers (Figure 1), expecting that these molecules would localize in different domains of the cell.

- (14) Snyder, J. W.; Skovsen, E.; Lambert, J. D. C.; Ogilby, P. R. *J. Am. Chem. Soc.* **2005**, *127*, 14558–14559.
- (15) Snyder, J. W.; Skovsen, E.; Lambert, J. D. C.; Poulsen, L.; Ogilby, P. R. *Phys. Chem. Chem. Phys.* **2006**, *8*, 4280–4293.
- (16) Hatz, S.; Lambert, J. D. C.; Ogilby, P. R. *Photochem. Photobiol. Sci.* **2007**, *6*, 1106–1116.
- (17) Snyder, J. W.; Zebger, I.; Gao, Z.; Poulsen, L.; Frederiksen, P. K.; Skovsen, E.; McIlroy, S. P.; Klinger, M.; Andersen, L. K.; Ogilby, P. R. *Acc. Chem. Res.* **2004**, *37*, 894–901.
- (18) Skovsen, E.; Snyder, J. W.; Ogilby, P. R. *Photochem. Photobiol.* **2006**, *82*, 1187–1197.
- (19) Ogilby, P. R.; Foote, C. S. *J. Am. Chem. Soc.* **1983**, *105*, 3423–3430.
- (20) Egorov, S. Y.; Kamalov, V. F.; Koroteev, N. I.; Krasnovsky, A. A.; Toleutaev, B. N.; Zinukov, S. V. *Chem. Phys. Lett.* **1989**, *163*, 421–424.
- (21) Ogilby, P. R. *Acc. Chem. Res.* **1999**, *32*, 512–519.
- (22) Breitenbach, T.; Kuimova, M. K.; Gbur, P.; Hatz, S.; Schack, N. B.; Pedersen, B. W.; Lambert, J. D. C.; Poulsen, L.; Ogilby, P. R. *Photochem. Photobiol. Sci.* [Online early access]. DOI: 10.1039/b809049a. Published Online: Sept 23, 2008.
- (23) By definition, the cytoplasm is the non-nuclear portion of a cell; it contains a multitude of organelles suspended in the so-called cytosol.
- (24) Kao, H. P.; Abney, J. R.; Verkman, A. S. *J. Cell Biol.* **1993**, *120*, 175–184.
- (25) Uchida, K.; Matsuyama, K.; Tanaka, K.; Doi, K. *Respir. Physiol.* **1992**, *90*, 351–362.
- (26) Dutta, A.; Popel, A. S. *J. Theor. Biol.* **1995**, *176*, 433–445.
- (27) Sidell, B. D. *J. Exp. Biol.* **1998**, *201*, 1118–1127.
- (28) Hatz, S.; Poulsen, L.; Ogilby, P. R. *Photochem. Photobiol.* **2008**, *84*, 1284–1290.

- (29) Kuimova, M. K.; Yahioglu, G.; Levitt, J. A.; Suhling, K. *J. Am. Chem. Soc.* **2008**, *130*, 6672–6673.

Materials and Methods

Cell Preparation and Handling. HeLa cells were cultured and maintained using methods described in detail elsewhere.¹⁶

For experiments in which singlet oxygen phosphorescence was detected from single cells, we continued to exploit the advantage of exchanging the intracellular H₂O with D₂O, which results in a larger quantum efficiency of singlet oxygen emission. Although we have found that it is no longer necessary to have complete exchange of the H₂O with D₂O (i.e., reasonable singlet oxygen signals can now be observed from cells containing up to 50% H₂O),^{15,16} it is still desirable to work with cells containing D₂O. The protocol for this H₂O/D₂O exchange is based on osmotic shock and has likewise been described previously.¹⁶ Since the intracellular singlet oxygen lifetimes we have measured depend linearly on the H₂O/D₂O ratio in the incubating medium and the plots extrapolate to a lifetime that is very close to that seen in neat H₂O,^{15,16} we expect homogeneous replacement of intracellular H₂O by D₂O.

Experiments were performed using cells exposed to an atmosphere of 100% oxygen, a condition that results in the most intense singlet oxygen phosphorescence signal.^{15,28}

Sensitizers were incorporated into the cells by incubating the cells in a medium that contained 10 μ M of the dye, as previously described.¹⁶ For Chl, a 1 mM stock solution of the dye in DMSO was diluted to a final concentration of 10 μ M in the incubation medium. The small amount of DMSO present in this case (1%) facilitated the incorporation of the hydrophobic Chl. At present, it is difficult to assess the concentration of the sensitizer when it is localized in a given subcellular domain.

Although sodium azide (NaN₃) is known to be toxic to cells,³⁰ such toxicity was not manifested in our measurements on azide-containing cells. Specifically, the combined time over which cells were incubated with sodium azide and the data recorded never exceeded 1.0–1.5 h. Viability assays (annexin V apoptosis assay and trypan blue exclusion assay for necrosis) performed on our cells showed no adverse effects of sodium azide over this period of time.

TMPyP, NaN₃, and sucrose were obtained from Sigma-Aldrich and used as received. Chl was synthesized as previously described.^{31,32}

Instrumentation. Details of the instrumentation and approach used in this study are provided elsewhere.^{13–15,18,33} Briefly, cells to be studied were contained in an atmosphere-controlled chamber that was mounted on the translation stage of an inverted microscope. Subsequent steps of irradiation and optical monitoring varied depending on the experiment.

For all of the kinetics experiments, the sensitizer that had been incorporated into the cell was irradiated using the output of a femtosecond laser system that had been focused into the cell using the microscope objective. The light emitted, be it singlet oxygen phosphorescence or sensitizer phosphorescence, was collected using the microscope objective, spectrally isolated using an interference filter, and transmitted to a cooled photomultiplier tube operated in a photon-counting mode. In a typical experiment, excitation energies ranged from 3 to 10 nJ/pulse at a repetition rate of 1 kHz.

Cell imaging was performed by irradiating the entire cell and its surroundings with a steady-state Xe lamp using interference filters to select the appropriate excitation wavelength. Light emitted by the sample was detected through interference filters using a CCD camera (Evolution QEi controlled by ImagePro software, Media Cybernetics) placed at the image plane of the microscope. Bright-field images were recorded using the same CCD camera, and back-

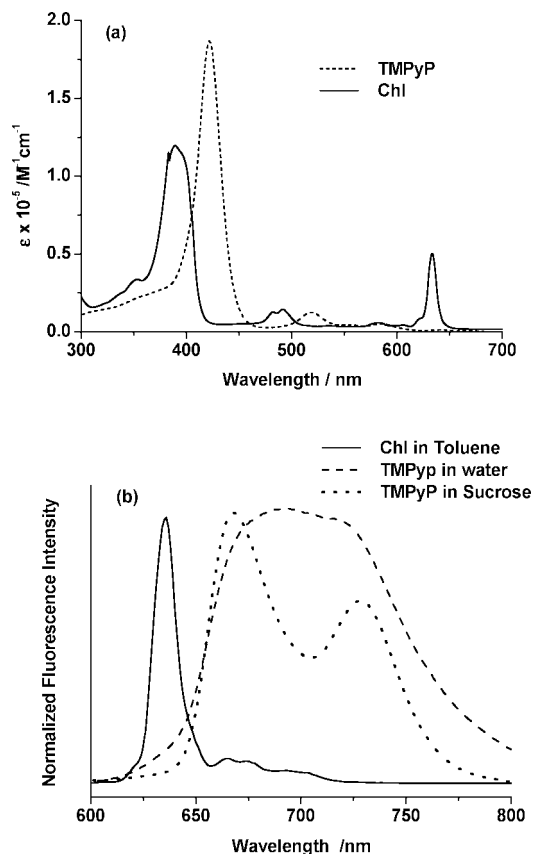


Figure 2. (a) Absorption and (b) fluorescence spectra of TMPyP in H₂O and Chl in toluene. Also shown is the fluorescence spectrum of TMPyP recorded in 1 M aqueous sucrose solution.

lighting was achieved with a tungsten lamp provided as an accessory to the Olympus IX70 inverted microscope.

Singlet oxygen quantum yields were obtained in bulk solution-phase experiments by comparing the intensity of the singlet oxygen phosphorescence recorded from the sensitizer in question to that obtained from a sensitizer standard, using an approach that has been described elsewhere.³⁴

Results and Discussion

1. General Characterization of TMPyP and Chl. TMPyP is a water-soluble photosensitizer that has a comparatively large quantum yield of singlet oxygen production, $\phi_{\Delta} = 0.77 \pm 0.04$.³⁵ The absorption spectrum of TMPyP, which is typical of porphyrins, is shown in Figure 2. Singlet oxygen can be produced upon irradiation into either the intense Soret band at ~ 420 nm or the weaker Q-band system over the range 500–600 nm. Also shown in Figure 2 are fluorescence spectra for TMPyP in water and in an aqueous sucrose solution. The differences in these emission spectra are consistent with what has been observed for TMPyP dissolved in water and methanol and, as examined and discussed in detail elsewhere,³⁶ likely reflect solvent-dependent phenomena rather than aggregation. Most importantly, the singlet oxygen kinetic data that we record (see

(30) Leary, S. C.; Hill, B. C.; Lyons, C. N.; Carlson, C. G.; Michaud, D.; Kraft, C. S.; Ko, K.; Glerum, D. M.; Moyes, C. D. *J. Biol. Chem.* **2002**, *277*, 11321–11328.

(31) Laha, J. K.; Muthiah, C.; Taniguchi, M.; McDowell, B. E.; Ptaszek, M.; Lindsey, J. S. *J. Org. Chem.* **2006**, *71*, 4092–4102.

(32) Taniguchi, M.; Ptaszek, M.; McDowell, B. E.; Lindsey, J. S. *Tetrahedron* **2007**, *63*, 3840–3849.

(33) Arnbjerg, J.; Johnsen, M.; Frederiksen, P. K.; Braslavsky, S. E.; Ogilby, P. R. *J. Phys. Chem. A* **2006**, *110*, 7375–7385.

(34) Scurlock, R. D.; Nonell, S.; Braslavsky, S. E.; Ogilby, P. R. *J. Phys. Chem.* **1995**, *99*, 3521–3526.

(35) Frederiksen, P. K.; McIlroy, S. P.; Nielsen, C. B.; Nikolajsen, L.; Skovsen, E.; Jørgensen, M.; Mikkelsen, K. V.; Ogilby, P. R. *J. Am. Chem. Soc.* **2005**, *127*, 255–269.

(36) Vergeldt, F. J.; Koehorst, R. B. M.; van Hoek, A.; Schaafsma, T. J. *J. Phys. Chem.* **1995**, *99*, 4397–4405.

section 2) do not depend on phenomena that influence these emission spectra.

TMPyP is readily incorporated into a cell upon incubation of the cell in a medium that contains TMPyP.¹⁶ Upon initial incorporation, TMPyP is first localized in lysosomes.^{37,38} However, the dye eventually localizes in the nucleus (Figure 3a).^{22,39} Under our cell-handling conditions, experiments were invariably initiated with an intracellular TMPyP distribution such as that shown in Figure 3a.

Chlorins are a class of porphyrin-like compounds containing one pyrrole ring that is reduced at the β -position. For our present study, we opted to use the parent, unsubstituted chlorin Chl, which is lipophilic (Figure 1). The absorption spectrum of this compound (Figure 2) shows the characteristic features that in general distinguish chlorins from porphyrins.⁴⁰ We have determined that the singlet oxygen quantum yield of Chl in toluene is $\phi_{\Delta} = 0.44 \pm 0.05$ (as obtained by monitoring the intensity of singlet oxygen phosphorescence using porphine, $\phi_{\Delta} = 0.67 \pm 0.06$, as the standard sensitizer⁴¹).

Upon incorporation into a cell, Chl clearly localizes outside the nucleus in the cell cytoplasm, with a distribution that appears to be quite inhomogeneous (Figure 3b). At present, we have not been able to determine the exact organelles and/or structures in the cytoplasm with which this hydrophobic dye associates. Nevertheless, and most importantly, the intracellular distribution of Chl is strikingly different from that of TMPyP.

2. Singlet Oxygen Quenching by Sodium Azide in Sucrose Solutions Having Different Viscosities. As discussed in the Introduction, there is considerable evidence to indicate that subcellular domains can be quite viscous. With this in mind, and prior to discussing data recorded from single cells, we present results obtained from bulk aqueous solutions of sucrose. By changing the concentration of sucrose in water, one obtains solutions in which viscosity and oxygen solubility can be varied over a wide range.^{42,43} More importantly, these sucrose-concentration-dependent changes in viscosity and oxygen solubility have been well-quantified.^{42,43} Consequently, singlet oxygen quenching experiments performed in sucrose solutions can be used to establish a reference framework for data recorded from a cell.

The molecule we have chosen as a singlet oxygen quencher for these studies is sodium azide, which readily penetrates cell membranes.³⁰ It is well established that NaN_3 is a good quencher of singlet oxygen. Values of the quenching rate constant, k_q , over the range $\sim 3\text{--}6 \times 10^8 \text{ s}^{-1} \text{ M}^{-1}$ have been reported for experiments performed in aqueous systems, and a value as large as $5 \times 10^9 \text{ s}^{-1} \text{ M}^{-1}$ has been reported for CH_3CN .⁴⁴ Although these values of k_q are slightly less than the rate constant value expected for a diffusion-limited process in a solvent whose viscosity is $\sim 1 \text{ mPa s}$ (i.e., $k_{\text{diff}} \approx 1\text{--}3 \times 10^{10} \text{ s}^{-1} \text{ M}^{-1}$),⁴⁵ the

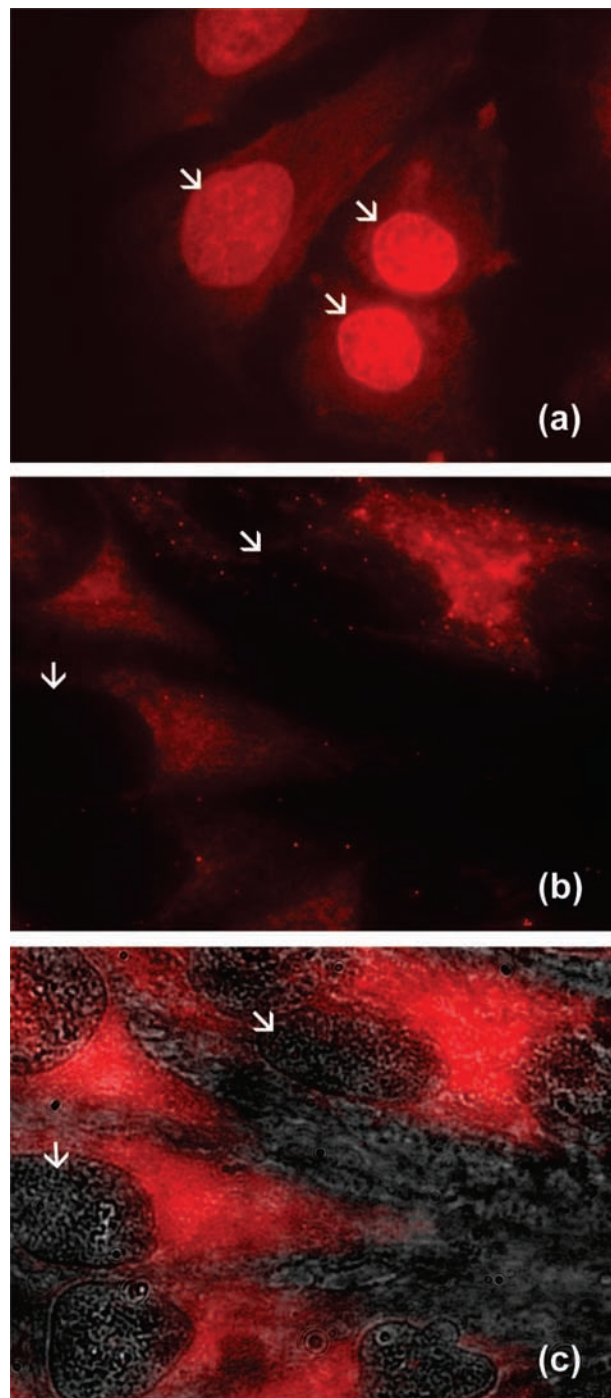


Figure 3. (a) Image of HeLa cells based on the fluorescence of TMPyP, showing the preference of this sensitizer to localize principally in the nucleus (white arrows). (b) Image of HeLa cells based on the fluorescence of Chl, showing the preference of this sensitizer to localize in the cytoplasm. Dark spots (white arrows) are the nuclei. (c) Overlay of the Chl fluorescence image in (b) with a transmission image that better shows the position of the nuclei (white arrows). Each image displays an area of $90 \mu\text{m} \times 65 \mu\text{m}$.

quenching of singlet oxygen by NaN_3 should readily approach the diffusion-controlled limit as the viscosity of the surrounding medium is increased. Although this viscosity-dependent phenomenon is general, it has been explicitly demonstrated for the quenching of singlet oxygen in a number of polymer-based

- (37) Patito, I. A.; Rothmann, C.; Malik, Z. *Biol. Cell* **2001**, *93*, 285–291.
 (38) Rück, A.; Köllner, T.; Dietrich, A.; Strauss, W.; Schneckenburger, H. *J. Photochem. Photobiol., B* **1992**, *12*, 403–412.
 (39) Snyder, J. W.; Lambert, J. D. C.; Ogilby, P. R. *Photochem. Photobiol.* **2006**, *82*, 177–184.
 (40) Gouterman, M. In *The Porphyrins*; Dolphin, D., Ed.; Academic Press: New York, 1978; Vol. 3, pp 1–165.
 (41) Ganzha, V. A.; Gurinovich, G. P.; Dzhagarov, B. M.; Egorova, G. D.; Sagun, E. I.; Shul'ga, A. M. *J. Appl. Spectrosc.* **1989**, *50*, 402–406.
 (42) Rischbieter, E.; Schumpe, A. *J. Chem. Eng. Data* **1996**, *41*, 809–812.
 (43) Mathlouthi, M.; Genotelle, J. In *Sucrose: Properties and Applications*; Mathlouthi, M., Reiser, P., Eds.; Blackie: London, U.K., 1994; pp 126–154.
 (44) Wilkinson, F.; Helman, W. P.; Ross, A. B. *J. Phys. Chem. Ref. Data* **1995**, *24*, 663–1021.

- (45) Ware, W. R. *J. Phys. Chem.* **1962**, *66*, 455–458.

systems.^{46–48} We now quantify the phenomenon in aqueous liquid-phase systems suitable for comparison to data recorded from cells.

We monitored the viscosity-dependent rate of singlet oxygen quenching by NaN_3 using the time-resolved 1270 nm phosphorescence of singlet oxygen as an experimental probe. For the triplet-state-photosensitized production of singlet oxygen, the evolution of the phosphorescence signal, P , with time should follow eq 1:^{15,20,49,50}

$$P(t) = \frac{K}{k_{\text{rem}} - k_{\text{T}}} (e^{-k_{\text{T}}t} - e^{-k_{\text{rem}}t}) \quad (1)$$

where K is a scaling parameter that includes the efficiency of singlet oxygen production, k_{T} is the rate constant for all channels of sensitizer triplet state deactivation, and k_{rem} is the rate constant that accounts for all channels of singlet oxygen removal. In our experiments, the latter can be expressed as the sum of three terms (eq 2):

$$k_{\text{rem}} = k_{\text{d}} + k_{\text{s}}[\text{S}] + k_{\text{q}}[\text{Q}] \quad (2)$$

where k_{d} is the pseudo-first-order rate constant for solvent-induced deactivation (i.e., quenching by water), $k_{\text{s}}[\text{S}]$ accounts for quenching by the sucrose added to change the viscosity of the solution, and $k_{\text{q}}[\text{Q}]$ accounts for quenching by any other molecules (i.e., in this case, added NaN_3). It should be noted that in aqueous and hydrocarbon systems, the rate constant for singlet oxygen radiative deactivation is small ($\sim 0.1\text{--}1.0\text{ s}^{-1}$)⁵¹ compared with the rate constants for the other deactivation channels and as such has not been included in the expression for k_{rem} . A rate constant for singlet oxygen quenching by sucrose has been published ($k_{\text{s}} = 2.5 \times 10^4\text{ s}^{-1}\text{ M}^{-1}$),⁵² and we have independently confirmed this value in our present experiments (see below). Although the latter is comparatively small (i.e., far removed from those in the diffusion-controlled regime), it can still be influenced by a change in viscosity.^{46,47}

In systems such as ours, where $k_{\text{T}} \approx k_{\text{rem}}$, the observed phosphorescence signal indeed appears as a difference of two exponential functions. In the analysis of such data, one cannot a priori assign the rising portion of the observed signal to k_{T} and the falling portion of the signal to k_{rem} . Rather, independent experiments and/or tests must be used to ascertain the rate-limiting step in the overall time evolution of the 1270 nm phosphorescence signal. This is often done in time-resolved experiments to quantify k_{T} (i.e., sensitizer triplet absorption or phosphorescence measurements). It is also well-established that (i) changes in the concentration of dissolved oxygen influence only k_{T} and not k_{rem} (the only exception occurring in solvents where the inherent lifetime of singlet oxygen is extraordinarily long, e.g., CCl_4 and CS_2) and (ii) changes in the H/D isotopic composition of the surrounding medium influence only k_{rem} and not k_{T} .^{2,15} In the present study, we used both direct triplet state measurements and H/D isotopic exchange to assign the rising and decaying portions of the signal to either k_{T} or k_{rem} .

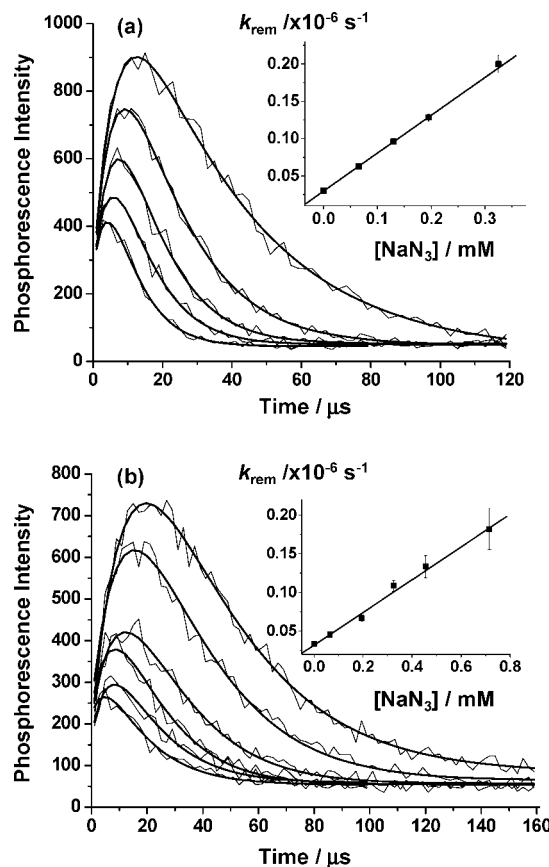


Figure 4. Time-resolved 1270 nm singlet oxygen phosphorescence traces recorded upon pulsed laser irradiation of TMPyP in air-saturated D_2O solutions containing (a) 0.88 and (b) 1.96 M sucrose. At these sucrose concentrations, $[\text{O}_2] = 0.84$ and 0.45 mM , respectively.⁴² In each case, data were recorded with different concentrations of added NaN_3 . The solid lines show fits of eq 1 to the data. The insets show plots of the rate constant for singlet oxygen removal, k_{rem} , against the concentration of NaN_3 (i.e., eq 2).

Time-resolved singlet oxygen phosphorescence signals were monitored as a function of NaN_3 concentration in aqueous solutions containing different amounts of sucrose. Data recorded in solutions of 0.88 M (2.4 mPa s) and 1.96 M (19 mPa s) sucrose are shown in Figure 4. Equation 1 was used as a fitting function for the time-resolved signals. The observed phosphorescence signals responded as expected, allowing us to clearly assign values of k_{T} and k_{rem} to a given time-resolved trace.

With an increase in the amount of added sucrose, and the corresponding increase in viscosity and decrease in oxygen solubility,^{42,43} the rate of sensitizer triplet state decay decreases, reflecting a decrease in the rate of bimolecular quenching by ground-state oxygen. When the values of k_{rem} obtained from the fits of eq 1 to the data were plotted against the sucrose concentration according to eq 2, we obtained a k_{s} value of $(1.8 \pm 0.2) \times 10^4\text{ s}^{-1}\text{ M}^{-1}$, which is consistent with published data (see above).

For all of the singlet oxygen phosphorescence traces recorded in a solution of the same viscosity (i.e., at a given sucrose concentration), the first-order rate constant for singlet oxygen decay (k_{rem}) increases with an increase in the NaN_3 concentration, whereas the rate constant for sensitizer triplet state decay (k_{T}) remains constant. This is entirely consistent with the expectation that NaN_3 does not efficiently quench the sensitizer

(46) Ogilby, P. R.; Dillon, M. P.; Kristiansen, M.; Clough, R. L. *Macromolecules* **1992**, *25*, 3399–3405.

(47) Scurlock, R. D.; Kristiansen, M.; Ogilby, P. R.; Taylor, V. L.; Clough, R. L. *Polym. Degrad. Stab.* **1998**, *60*, 145–159.

(48) Turro, N. J.; Chow, M.-F.; Blaustein, M. A. *J. Phys. Chem.* **1981**, *85*, 3014–3018.

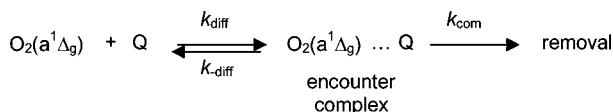
(49) Baier, J.; Maier, M.; Engl, R.; Landthaler, M.; Bäuml, W. *J. Phys. Chem. B* **2005**, *109*, 3041–3046.

(50) Jiménez-Banzo, A.; Sagrista, M. L.; Mora, M.; Nonell, S. *Free Radical Biol. Med.* **2008**, *44*, 1926–1934.

(51) Poulsen, T. D.; Ogilby, P. R.; Mikkelsen, K. V. *J. Phys. Chem. A* **1998**, *102*, 9829–9832.

(52) Egorov, S. Y.; Krasnovsky, A. A. *Sov. Plant Physiol.* **1986**, *33*, 5–8.

Scheme 1. General Kinetic Scheme Used to Model Singlet Oxygen Removal by a Quencher Q, Where k_{diff} and $k_{-\text{diff}}$ Are the Rate Constants for Diffusion-Limited Processes



triplet state.⁵³ In support of this latter expectation, we independently monitored the decay rate of TMPyP phosphorescence in sucrose-free D₂O as a function of added NaN₃ and obtained a bimolecular quenching rate constant of $(1.3 \pm 0.1) \times 10^5 \text{ s}^{-1} \text{ M}^{-1}$, which is indeed much smaller than the rate constant for singlet oxygen quenching by NaN₃. In the limit of a highly viscous solution (e.g., 1.96 M sucrose), increasing the azide concentration leads to a reversal in the magnitude of the rate constants in eq 1 (i.e., $k_{\text{rem}} > k_{\text{T}}$). Under these conditions, the rate of sensitizer triplet state deactivation is principally responsible for the falling part of the observed time-resolved signal, while the singlet oxygen decay is manifested on the rising part (Figure 4b).

Values of k_{rem} obtained from our fits to the time-resolved traces were plotted against the concentration of added azide (i.e., eq 2) to yield values for the bimolecular rate constant k_{q} for singlet oxygen quenching by NaN₃ (see the insets in Figure 4). The value we obtained in sucrose-free D₂O, $(5.1 \pm 0.1) \times 10^8 \text{ s}^{-1} \text{ M}^{-1}$, agrees well with previously published values of k_{q} in aqueous environments.⁴⁴

Before the viscosity dependence of singlet oxygen quenching by NaN₃ is discussed, it is useful to be reminded of the general model that describes singlet oxygen quenching.^{46,54} As with many other species, singlet oxygen removal can be considered to occur in two steps: (i) reversible diffusion in which an encounter complex is formed, and (ii) chemical/physical interactions within the encounter complex that result in removal (Scheme 1). On the basis of this kinetic scheme, the overall quenching rate constant k_{q} that would be obtained experimentally is described by eq 3:⁵⁵

$$k_{\text{q}} = \frac{k_{\text{diff}}k_{\text{com}}}{k_{-\text{diff}} + k_{\text{com}}} \quad (3)$$

Two limiting conditions occur: (i) when $k_{\text{com}} \gg k_{-\text{diff}}$, quenching will be determined by solute diffusion to form the encounter complex, and $k_{\text{q}} = k_{\text{diff}}$; (ii) when $k_{\text{com}} \ll k_{-\text{diff}}$, events that occur within the encounter pair will be rate-determining, and $k_{\text{q}} = (k_{\text{diff}}/k_{-\text{diff}})k_{\text{com}}$. The latter case defines the so-called reaction or pre-equilibrium limit.⁵⁵

In Figure 5, values of k_{q} for the quenching of singlet oxygen by NaN₃ obtained from plots of eq 2 for the various sucrose concentrations are plotted against the reciprocal of the solution viscosity. This plot illustrates that there are two distinct viscosity-dependent regimes in the reaction between singlet oxygen and NaN₃. At low viscosities, the rate of singlet oxygen deactivation is determined by the pre-equilibrium condition. This is consistent with the behavior of many singlet oxygen quenchers.^{47,54} As the solution viscosity is increased, however,

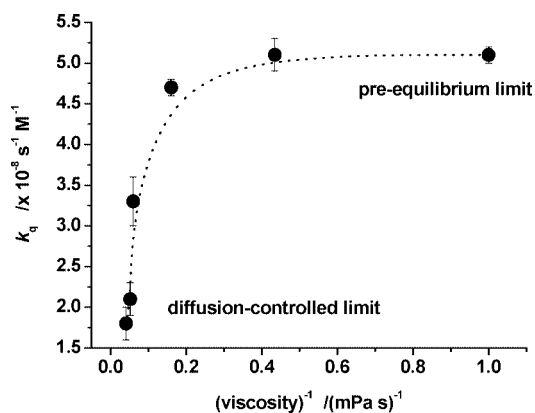


Figure 5. Rate constants for singlet oxygen quenching by NaN₃ in six different aqueous sucrose solutions plotted against the reciprocal of the solution viscosity.

the magnitude of the bimolecular quenching rate constant decreases, indicating that the process of singlet oxygen deactivation is now determined by the rate at which singlet oxygen and NaN₃ encounter each other (i.e., the diffusion-controlled limit).

Since the apparent intracellular diffusion coefficient for a small molecule such as oxygen can be comparatively small^{25–28} and subcellular domains can have apparent viscosities that are comparatively large,²⁹ the data shown in Figure 5 provide the necessary framework to interpret the data recorded upon quenching of intracellular singlet oxygen by NaN₃. We note here that while the intracellular matrix is intrinsically heterogeneous, it is expected that on a microscopic scale, homogeneous domains will exist.²⁹ (In this way, Figure 5 is still a pertinent reference.) The intent in our intracellular experiments is to probe the diffusion-dependent behavior of singlet oxygen kinetics in these microscopic domains.

3. Singlet Oxygen Production and Quenching by NaN₃ in Cells with TMPyP as the Sensitizer. When incorporated into HeLa cells, TMPyP ultimately tends to localize in the nucleus, where it most likely binds to DNA (Figure 3a).^{39,56,57} Nevertheless, appreciable amounts of this hydrophilic dye appear in the cytoplasm. At present, it is unclear whether extra-nuclear TMPyP freely diffuses in the cytosol or if it binds, for example, to proteins.^{58,59}

Upon irradiation of TMPyP in these respective intracellular domains, we were able to record time-resolved singlet oxygen phosphorescence signals. It should be noted that the cross-sectional diameter of the irradiating laser beam ($\sim 1 \mu\text{m}$) was large relative to microscopic intracellular structures. Singlet oxygen signals recorded from the nucleus of a HeLa cell are shown in Figure 6a. The absence of a visible rising component in our signals is consistent with the high oxygen concentration used in these experiments (i.e., k_{T} is comparatively large). Data were recorded from cells that had been exposed to a buffered medium containing concentrations of NaN₃ ranging from 0 to 0.7 mM and clearly show a significant NaN₃-dependent increase in the rate of singlet oxygen decay. Similar data were recorded upon irradiation of TMPyP in the cytoplasm of HeLa cells.

(53) Nilsson, R.; Kearns, D. R.; Merkel, P. B. *Photochem. Photobiol.* **1972**, *16*, 109–116.

(54) Gorman, A. A.; Hamblett, I.; Lambert, C.; Spencer, B.; Standen, M. C. *J. Am. Chem. Soc.* **1988**, *110*, 8053–8059.

(55) Rice, S. A. In *Comprehensive Chemical Kinetics*; Bamford, C. H., Tipper, C. F. H., Compton, R. G., Eds.; Elsevier: New York, 1985; Vol. 25, pp 1–404.

(56) Kruk, N. N.; Dzhagarov, B. M.; Galievsky, V. A.; Chirvony, V. S.; Turpin, P.-Y. *J. Photochem. Photobiol., B* **1998**, *42*, 181–190.

(57) Borissevitch, I. E.; Gandini, S. *J. Photochem. Photobiol., B* **1998**, *43*, 112–120.

(58) Borissevitch, I. E.; Tominaga, T. T.; Schmitt, C. C. *J. Photochem. Photobiol., A* **1998**, *114*, 201–207.

(59) Lang, K.; Mosinger, J.; Wagnerova, D. M. *Coord. Chem. Rev.* **2004**, *248*, 321–350.

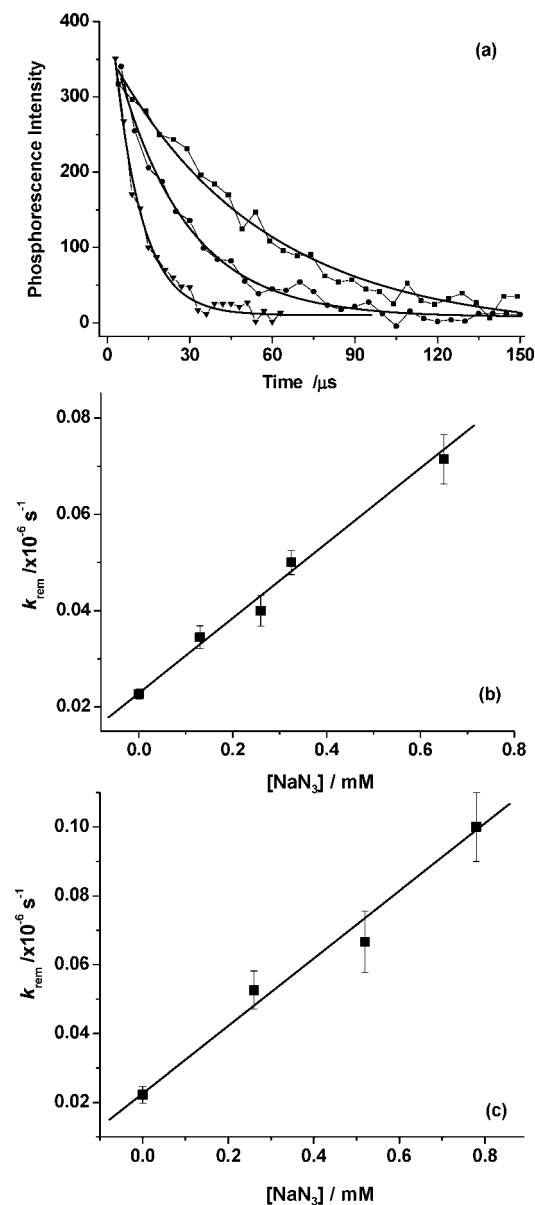


Figure 6. (a) Time-resolved singlet oxygen phosphorescence traces recorded at 1270 nm upon irradiation of TMPyP in the nucleus of oxygen-saturated HeLa cells. Data are shown for cells that had been exposed to a medium containing (■) 0, (●) 0.13, and (▲) 0.65 mM NaN_3 . The lower panels show plots of the rate constant for singlet oxygen removal, k_{rem} , against the concentration of NaN_3 in the incubating medium for data recorded from (b) the nucleus and (c) the cytoplasm.

For these intracellular experiments, the rate constant that accounts for all channels of singlet oxygen removal, k_{rem} , can be expressed as a sum of four terms (eq 4):

$$k_{\text{rem}} = k_{\text{d}}^{\text{H}}[\text{H}_2\text{O}] + k_{\text{d}}^{\text{D}}[\text{D}_2\text{O}] + k_{\text{c}}[\text{C}] + k_{\text{q}}[\text{Q}] \quad (4)$$

where $k_{\text{d}}^{\text{H}}[\text{H}_2\text{O}]$ and $k_{\text{d}}^{\text{D}}[\text{D}_2\text{O}]$ are the pseudo-first-order rate constants for H_2O - and D_2O -induced deactivation, respectively. The relative contribution of these two terms depends on the extent of $\text{H}_2\text{O}/\text{D}_2\text{O}$ exchange in the cell. The third term, $k_{\text{c}}[\text{C}]$, represents all channels for singlet oxygen removal by components inherent to the cell (e.g., proteins, DNA). The final term, $k_{\text{q}}[\text{Q}]$, accounts for quenching by added NaN_3 .

The lifetimes (i.e., values of $1/k_{\text{rem}}$) obtained in the absence of added NaN_3 are consistent with those previously reported.^{13–16} Specifically, for D_2O -incubated cells, we repeatedly found that

the lifetimes determined both in the cytoplasm and in the nucleus ($\sim 30\text{--}40 \mu\text{s}$) are shorter than that for singlet oxygen in pure D_2O ($67 \mu\text{s}$). These data point to a non-negligible $k_{\text{c}}[\text{C}]$ term,^{13–16} as is indeed expected given that singlet oxygen can induce cell death. The quenching plots obtained using the NaN_3 -dependent lifetime data (shown in Figure 6b,c) yield $k_{\text{q}}(\text{nucleus}) = (7.8 \pm 0.7) \times 10^7 \text{ s}^{-1} \text{ M}^{-1}$ and $k_{\text{q}}(\text{cytoplasm}) = (1.0 \pm 0.1) \times 10^8 \text{ s}^{-1} \text{ M}^{-1}$ for irradiation of TMPyP localized in the nucleus and cytoplasm, respectively.

These rate constants for the quenching of intracellular singlet oxygen by NaN_3 are very similar to each other, and both are significantly smaller than the value obtained in neat D_2O , $k_{\text{q}} = (5.1 \pm 0.1) \times 10^8 \text{ s}^{-1} \text{ M}^{-1}$. If it is assumed that the intracellular concentration of NaN_3 equals the extracellular concentration in the incubating medium, the data in Figure 5 suggest that this intracellular quenching occurs at the diffusion-controlled limit. Moreover, in accordance with the calibration graph in Figure 5, the quenching rate constant of $(1.0 \pm 0.1) \times 10^8 \text{ s}^{-1} \text{ M}^{-1}$ corresponds to an apparent intracellular viscosity of $>25 \text{ mPa s}$. This conclusion is further strengthened by comparison with the results of singlet oxygen quenching by NaN_3 in Chl-sensitized experiments (see below).

4. Singlet Oxygen Production and Quenching by NaN_3 in Cells with Chl as the Sensitizer. As already discussed, the sensitizer Chl localizes in different intracellular domains than does TMPyP. Upon 390 nm pulsed laser irradiation of Chl in the cytoplasm, we were indeed able to observe a time-resolved emission signal at 1270 nm. However, since this was the first time Chl had been used in such an experiment, it was necessary to perform a few control experiments to ascertain that the signal we observed was indeed due to singlet oxygen phosphorescence.

First, although the phosphorescence spectrum of singlet oxygen depends slightly on solvent, the emission maximum is always $\sim 1270 \text{ nm}$, and there is no emission at 1200 nm .^{60,61} Indeed, we did not observe a signal at 1200 nm but saw an appreciable signal at 1270 nm upon irradiation of intracellular Chl. Second, we observed a 2-fold decrease in the intensity of our signal when the amount of oxygen in the ambient atmosphere was decreased from 100 to 60%, which is consistent with the expectation for intracellular singlet oxygen phosphorescence.²⁸ Third, upon successively increasing the intracellular $\text{H}_2\text{O}/\text{D}_2\text{O}$ ratio, we saw a corresponding successive increase in the decay rate of our signal (Figure 7). Although Chl is presumably located in lipophilic domains and the singlet oxygen produced would likewise be initially located in these domains, subsequent diffusion of singlet oxygen is expected to allow for appreciable encounter with aqueous domains. In light of this, it is not just reasonable but indeed expected that a $\text{H}_2\text{O}/\text{D}_2\text{O}$ solvent effect on such a singlet oxygen signal be seen.⁶² This point is discussed further below. Thus, in conclusion, we can assign the 1270 nm emission signal observed upon irradiation of intracellular Chl to singlet oxygen phosphorescence.

To further characterize the Chl-sensitized intracellular singlet oxygen system, we examined the decay kinetics of the Chl triplet state, which is the immediate precursor to singlet oxygen. Phosphorescence from free-base porphyrins is routinely observed with reasonable intensity over the wavelength range

(60) Macpherson, A. N.; Truscott, T. G.; Turner, P. H. *J. Chem. Soc., Faraday Trans.* **1994**, *90*, 1065–1072.

(61) Wessels, J. M.; Rodgers, M. A. *J. Phys. Chem.* **1995**, *99*, 17586–17592.

(62) Ehrenberg, B.; Anderson, J. L.; Foote, C. S. *Photochem. Photobiol.* **1998**, *68*, 135–140.

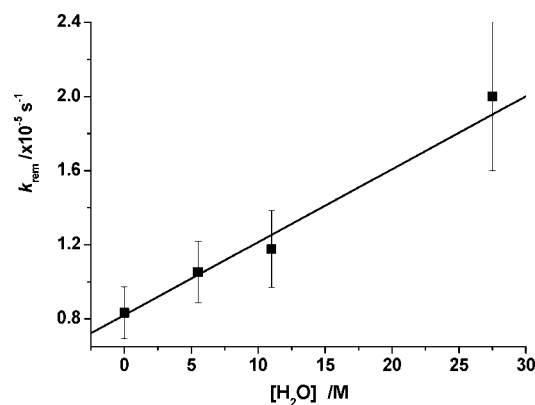


Figure 7. Plot of the rate constant for singlet oxygen removal, k_{rem} , against the concentration of H_2O in the D_2O -based medium used to incubate HeLa cells. The data were recorded upon irradiation of Chl that had been incorporated into the cells and indicate that the intracellular lifetime in this system is indeed sensitive to the intracellular $[\text{H}_2\text{O}]/[\text{D}_2\text{O}]$ ratio.

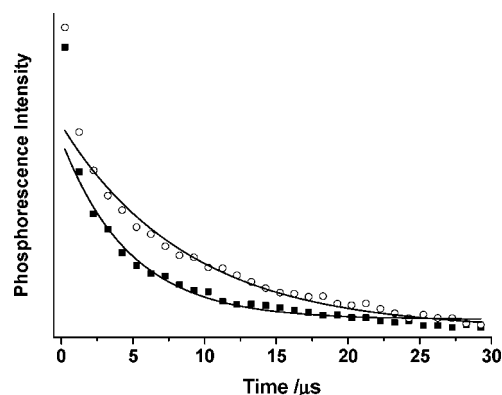


Figure 8. Time-resolved Chl phosphorescence decays recorded at 800 nm following irradiation of Chl in a HeLa cell exposed to (○) nitrogen-saturated and (■) air-saturated media. The first point in each data set is in a time domain in which our signal is characterized by the system response to scattered laser light ($\tau \approx 1.5 \mu\text{s}$), and these points have not been included in the exponential fits shown. Data were recorded from cells that had been incubated with a Chl-containing medium for 2 h.

$\sim 750\text{--}950 \text{ nm}$,⁴⁰ and this phosphorescence can even be observed from cells that contain an appreciable amount of oxygen.^{15,50} Chl phosphorescence was readily detected at 800 nm from our HeLa cells (Figure 8). Upon exposure of our cells to a nitrogen-saturated medium, intracellular ^3Chl decayed with a lifetime of $8.8 \pm 0.3 \mu\text{s}$. This comparatively short lifetime can be attributed to incomplete deoxygenation of the cell. Upon exposure to an atmosphere of air, the decay rate increased, yielding a lifetime of $4.8 \pm 0.3 \mu\text{s}$. Under an atmosphere of 100% oxygen, we could not differentiate between our instrument response to scattered light ($\tau \approx 1.5 \mu\text{s}$) and the Chl triplet state decay. The key point here is that under the conditions in which we observe our intracellular Chl-sensitized singlet oxygen signal (100% oxygen), we have no evidence of an intracellular population of ^3Chl with a lifetime longer than $4 \mu\text{s}$. This is manifested in our singlet oxygen signals by the apparent lack of a rising component (i.e., $k_{\text{T}} > k_{\text{rem}}$ in eq 1).

After a 2 h incubation of HeLa cells with a Chl-containing D_2O -based medium, we obtained a Chl-sensitized intracellular singlet oxygen lifetime of $17 \pm 2 \mu\text{s}$. It is important to note that this lifetime is appreciably shorter than those obtained when TMPyP was used as the sensitizer (see above). In itself, this is a significant observation; we are now able to provide evidence

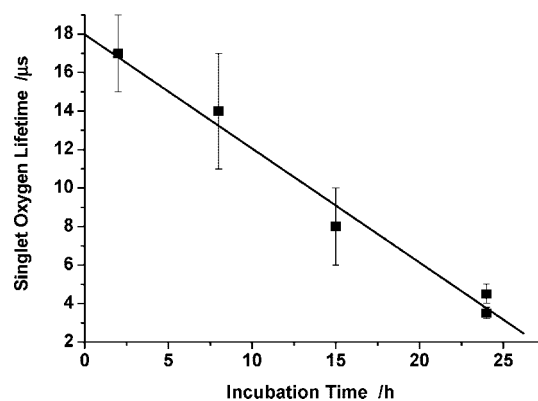


Figure 9. Singlet oxygen lifetime recorded upon irradiation of Chl incorporated into a HeLa cell as a function of the incubation time of the cell in a Chl-containing medium. The plot yields a limiting value of $18 \pm 1 \mu\text{s}$ for the lifetime at an incubation time of 0 h.

of sensitizer-dependent subcellular singlet oxygen lifetimes. Such differences in the lifetime of intracellular singlet oxygen could reflect different chemical compositions of cellular domains (i.e., different $k_{\text{c}}[\text{C}]$ terms in eq 4). These data could also reflect partitioning of singlet oxygen between hydrophobic and hydrophilic domains (e.g., one must also consider a hydrocarbon-derived solvent-dependent deactivation term, $k_{\text{d}}^{\text{hyd}}[\text{hyd}]$, in eq 4). In any case, this difference in lifetimes indicates that the environment of singlet oxygen produced by either TMPyP or Chl is unique to each photosensitizer.

The Chl-sensitized intracellular singlet oxygen data are also characterized by another unique feature: the decay kinetics of the singlet oxygen phosphorescence signal depends on the elapsed time with which the HeLa cells were incubated with the medium containing Chl (Figure 9). Specifically, we observed a marked decrease in the intracellular singlet oxygen lifetime as the incubation time with the Chl-containing medium was increased. After an incubation period of 24 h, we obtained a lifetime of $4.5 \pm 0.5 \mu\text{s}$. It is reasonable to assume that this dependence on the incubation time reflects the effect of singlet oxygen quenching by the sensitizer and that with an increased incubation period, the intracellular concentration of the sensitizer correspondingly increases (i.e., we must consider yet another term in eq 4, $k_{\text{sens}}[\text{sens}]$). We have indeed substantiated this latter point by ascertaining that the distribution pattern of the intracellular Chl fluorescence does not change with an increase in the incubation time, while the intensity of the intracellular fluorescence of Chl increases markedly with incubation time.

In an independent control experiment, we monitored the singlet oxygen lifetime in a bulk methanol solution as a function of the Chl concentration. We likewise found that the measured lifetime decreases with an increase in the Chl concentration. From these methanol data, we obtained a rate constant of $(9 \pm 2) \times 10^8 \text{ s}^{-1} \text{ M}^{-1}$ for the quenching of singlet oxygen by Chl at the limit of low Chl concentrations ($< 2 \times 10^{-5} \text{ M}$). This value is consistent with those reported for the quenching of singlet oxygen by other porphyrin-based systems.⁴⁴ If we assume that the magnitude of this rate constant does not change appreciably with solvent, then we can use it to estimate that an intracellular Chl concentration of $\sim 0.2 \text{ mM}$ would lead to the observed change in the singlet oxygen lifetime from 17 ± 2 to $4.5 \pm 0.5 \mu\text{s}$.

Time-resolved singlet oxygen phosphorescence signals were recorded from Chl-containing HeLa cells as a function of the NaN_3 concentration in the incubating medium to which the cells

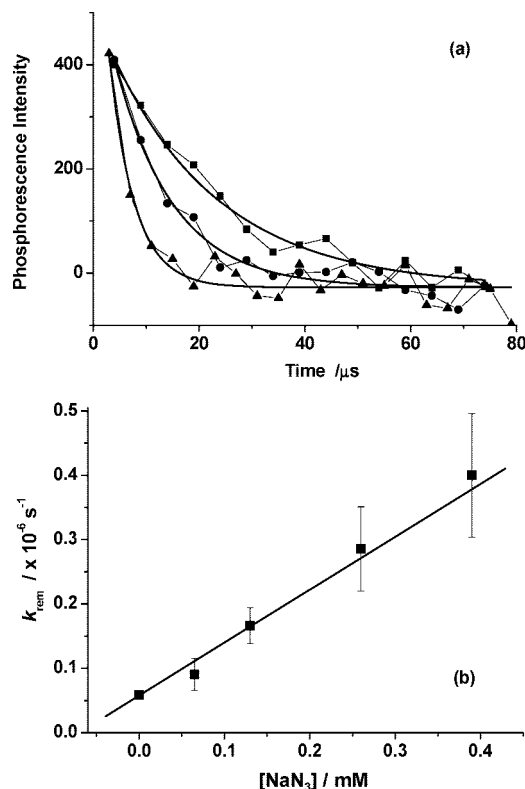


Figure 10. (a) Time-resolved singlet oxygen phosphorescence traces recorded at 1270 nm following irradiation of Chl in oxygen-saturated HeLa cells. Data are shown for cells that had been exposed to a medium containing (■) 0, (●) 0.065, and (▲) 0.26 mM NaN_3 . (b) Plot of the rate constant for singlet oxygen removal, k_{rem} , obtained from traces such as those shown in (a) against the concentration of NaN_3 in the incubating medium. The data yield a rate constant for the quenching of singlet oxygen by NaN_3 of $k_q = (8 \pm 1) \times 10^8 \text{ s}^{-1} \text{ M}^{-1}$.

had been exposed (Figure 10). These data were recorded using a 2 h incubation period for Chl incorporation. The quenching plot obtained using the NaN_3 -dependent lifetimes (i.e., eq 4) is shown in Figure 10b and yields $k_q = (8 \pm 1) \times 10^8 \text{ s}^{-1} \text{ M}^{-1}$. This value is significantly larger than those obtained in the TMPyP-photosensitized experiments [e.g., $k_q(\text{cytoplasm}) = (1.0 \pm 0.1) \times 10^8 \text{ s}^{-1} \text{ M}^{-1}$]. Moreover, the quenching constant obtained in this Chl-photosensitized experiment is slightly larger than the k_q value of $(5.1 \pm 0.1) \times 10^8 \text{ s}^{-1} \text{ M}^{-1}$ determined in a bulk D_2O solution (see above).

Explanations for the differences in the magnitudes of these NaN_3 quenching rate constants must start with the recognition

that with hydrophobic Chl and hydrophilic TMPyP, singlet oxygen is produced and presumably principally localized in different domains of the heterogeneous cellular matrix. This is consistent with our lifetime data (see above). Thus, it is reasonable to suggest that the average environments seen by singlet oxygen in these respective cases are different. On this basis, a very simplistic explanation for the NaN_3 quenching rate constant in the Chl-sensitized experiment is that in this case, an appreciable fraction of the singlet oxygen produced exists in a nonaqueous environment, so the difference between $k_q(\text{Chl})$ in a cell and $k_q(\text{bulk } \text{D}_2\text{O})$ would then reflect a solvent effect on k_q ; such an effect can be seen, for example, in a comparison of the k_q values for the reaction of singlet oxygen with NaN_3 in an aqueous environment ($\sim 4 \times 10^8 \text{ s}^{-1} \text{ M}^{-1}$) and in CH_3CN ($5 \times 10^9 \text{ s}^{-1} \text{ M}^{-1}$).⁴⁴

A more general explanation for the NaN_3 quenching data is that there could be domain-dependent local gradients in the intracellular NaN_3 concentration. However, the validity of this interpretation still relies on the significant fact that the diffusion of singlet oxygen from one subcellular domain to another must be restricted, principally as a result of a comparatively high intracellular viscosity.

Conclusions

Time-resolved singlet oxygen phosphorescence experiments were performed at the level of a single cell using sensitizers that localize in different subcellular domains. Sensitizer-dependent values for (i) the intracellular singlet oxygen lifetime and (ii) the rate constant for singlet oxygen quenching by added NaN_3 were obtained. The data are consistent with a model in which, irrespective of which sensitizer is used, singlet oxygen exists in intracellular domains that are more viscous than water at 25 °C. In view of its finite lifetime and viscosity-dependent diffusion coefficients that can be small, it appears that singlet oxygen can serve as a sensitive probe of the local environment. In short, we have demonstrated that singlet oxygen senses the inherent heterogeneity of a cell. This result has ramifications for issues ranging from cell death to mechanisms of oxygen-dependent signal transmission.

Acknowledgment. M.K.K. thanks the EPSRC Life Sciences Interface Programme (U.K.) for a fellowship. We thank Brian Wett Pedersen for assistance with cell viability studies. This work was supported by the Danish National Research Foundation under a block grant for the Center for Oxygen Microscopy and Imaging.

JA807484B